

Article

Development and Commissioning of a Small-Scale, Modular and Integrated Plant for the Quasi-Continuous Production of Crystalline Particles

Timo Dobler *, Simon Buchheiser, Marco Gleiß and Hermann Nirschl

Karlsruhe Institute of Technology (KIT), Institute of Mechanical Process Engineering and Mechanics, Strasse am Forum 8, 76131 Karlsruhe, Germany; uwdsy@student.kit.edu (S.B.); marco.gleiss@kit.edu (M.G.); hermann.nirschl@kit.edu (H.N.)

* Correspondence: timo.dobler@kit.edu; Tel.: +49-721-608-44136

Abstract: Increasing global competition, volatile markets and the demand for individual products challenge companies in almost all business sectors and require innovative solutions. In the chemical and pharmaceutical industries, these include modular design, the integration of several unit operations in one apparatus and the development of small-scale, versatile multipurpose plants. An example for such a modular, integrated and small-scale system is the belt crystallizer. This device combines the process steps cooling crystallization, solid-liquid separation and contact drying in a single plant. The basis of the apparatus is a belt filter in which the vacuum trays below the filter medium are replaced by temperature control and filtration units. Due to identical dimensions, it is possible to arrange the individual functional units in any order, which in turn allows a high degree of flexibility and rapid adaptation to customer requirements. Within the scope of the publication, the commissioning of the belt crystallizer takes place. First of all, the general functionality of the plant concept is demonstrated using sucrose as model system. Further experiments show that the particle size and the distribution width of the manufactured crystals can be specifically influenced by the selected process parameters, e.g., temperature profile during cooling and residence time.

Keywords: modularization; plant engineering; crystallization; solid-liquid separation; integrated process design



Citation: Dobler, T.; Buchheiser, S.; Gleiß, M.; Nirschl, H. Development and Commissioning of a Small-Scale, Modular and Integrated Plant for the Quasi-Continuous Production of Crystalline Particles. *Processes* **2021**, *9*, 663. <https://doi.org/10.3390/pr9040663>

Academic Editor: Luis Puigjaner

Received: 25 February 2021

Accepted: 7 April 2021

Published: 9 April 2021

Publisher's Note: MDPI stays neutral with regard to jurisdictional claims in published maps and institutional affiliations.



Copyright: © 2021 by the authors. Licensee MDPI, Basel, Switzerland. This article is an open access article distributed under the terms and conditions of the Creative Commons Attribution (CC BY) license (<https://creativecommons.org/licenses/by/4.0/>).

1. Introduction

In almost every industrial sector companies are faced with constantly changing challenges. In the chemical and pharmaceutical industry this includes increasing global competition, growing market volatility, short product life cycles and plant lifetimes as well as rising quality demands and the request for individual products in small amounts [1–4]. One approach to meet these challenges successfully and to ensure long-term business success is the establishment of adaptable, small-scale, modular production concepts that combine the flexibility and versatility of a discontinuous multi-product asset with the efficiency and reproducibility of a continuous single-product plant [2,4,5]. The modular design enables a reduction in time-to-market and controlled capacity adjustment along with simple and fast plant maintenance [6,7]. Further positive aspects are the decentralized production close to the customer, short retooling times in case of a product change and lower investment costs due to the recycling of modules [4,8–10]. Despite the advantages, modular production plants are still rarely used in the chemical industry. There are various reasons for this, ranging from the limitations of the technical possibilities due to design guidelines or conflicting goals to the additional construction effort [11]. However, one example that demonstrates the need for and the benefits of modular plants is the container-based production facility EvoTrainer. Evonik already deploys the concept successfully for rapid product development and for the small-scale production of chemicals [11].

In addition to modularization, the integration of different unit operations in one plant becomes more and more important. The main advantages are the reduction in transport facilities such as pumps, minimization of the risk of contamination, smaller space requirements and simplified implementation of safety standards, e.g., when using solvents. In contrast, optimizing the individual process steps is a challenge. Since these are usually linked to each other via predefined machine parameters, an intelligent system control and a high degree of automation are required to improve the overall process [12]. Despite this limitation, there are some integrated plants in the field of process engineering [13–16]. Among these are the Titus-Nutschen-Dryer [15] and the Konfilitro, which combines filtration and drying on a belt filter and serves as a basis for the apparatus concept presented in this publication [13,14]. Compared to the classic design of the Konfilitro, the newly developed plant consists of modular equipment and includes a cooling crystallization step in addition to filtration and drying. Thus, the apparatus combines the advantages of both modularization and integration and extends the application area, which reaches from the production to the separation of crystalline particles. To demonstrate the basic functionality of the plant, the initial commissioning is followed by tests with the system sucrose/water.

2. Materials and Methods

2.1. Belt Crystallizer

2.1.1. Apparatus Concept and Process Procedure

The belt crystallizer is a quasi-continuous apparatus, which includes the process steps cooling crystallization, solid-liquid separation and contact drying. The general working principle has already been described by Löbnitz [12]. The basis of the plant is a belt filter. In contrast to the conventional design, flexible and exchangeable functional units replace the vacuum trays below the filter medium. While there are temperature control segments in the crystallization zone, filtration modules are installed in the solid-liquid separation area. For drying the crystals, temperature control units are used again. The process chamber in which particle production takes place is located above the filter medium and passes through the process chain from left to right. Figure 1 shows the described apparatus concept schematically.

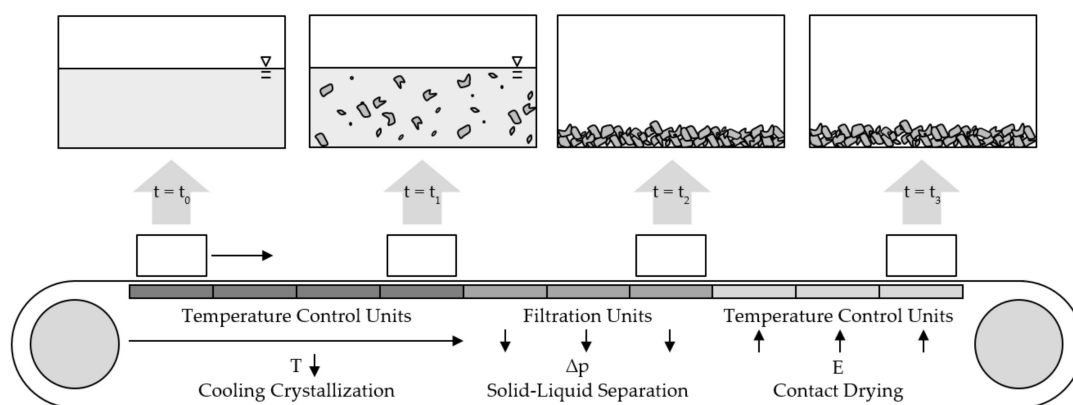


Figure 1. Apparatus concept and process procedure. At time $t = t_0$ there is an inoculated and saturated solution. By reducing the temperature T suspension has formed at $t = t_1$. The suspension is subsequently separated by an applied pressure difference Δp and leaves the solid-liquid separation zone at $t = t_2$. Due to the input of thermal energy E , only the dried product is left at $t = t_3$.

Referring to the same figure, the process procedure is explained. In a first step, an inoculated, saturated solution is added to the process chamber at time $t = t_0$ and subsequently cooled in the crystallization zone. This causes supersaturation in the system, which is reduced by the formation of crystalline particles ($t = t_1$). In the next stage, the solid and liquid components are separated by applying a vacuum and the resulting filter cake is mechanically demostriated ($t = t_2$). Optionally, an additional displacement washing

occurs within the same zone. The filter cake is then dried by the input of thermal energy and removed from the filter at time $t = t_3$.

2.1.2. Apparatus Implementation

The laboratory apparatus was a prototype and measured 1340 mm in length, 350 mm in width and 510 mm in height. It was controlled by a superordinate process control system. An image of the entire plant can be seen in Figure 2.

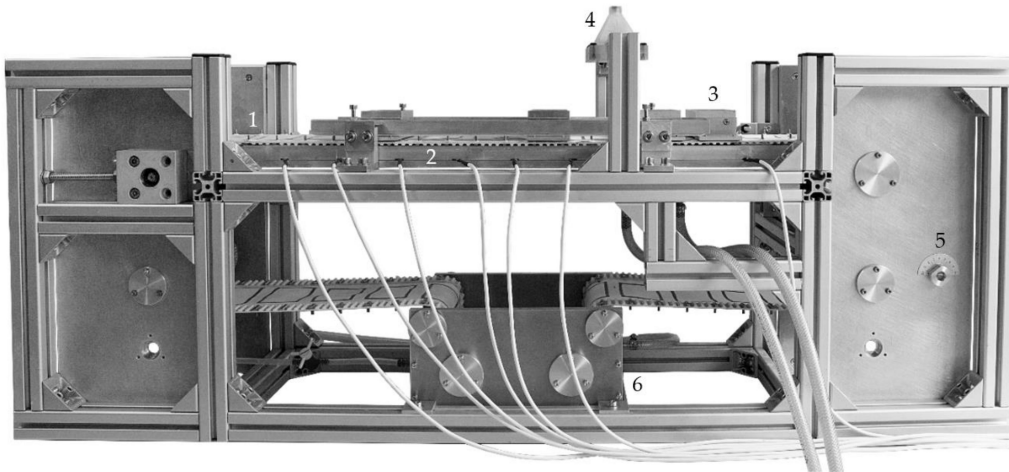


Figure 2. Laboratory apparatus. The plant consisted of flexible functional units (1), filter medium (2), process chamber (3), cake washing device (4), scraper (5) and washing tub (6).

Below the filter medium, the modified belt filter offered space for up to nine functional units. The basis of each functional unit was a 142 mm × 80 mm × 25 mm polyethylene frame. The low thermal conductivity of the plastic ensured that two units located next to each other were prevented from interaction. Depending on the area of application, different components were enclosed inside of the frame. In this context, the temperature control segments included a heating mat (RS Components GmbH, Frankfurt am Main, Germany), an aluminum plate and a thin stainless steel sheet. The sheet avoided contact between the aluminum and the product and hindered unwanted chemical reactions, such as oxidation processes. In addition to an aluminum tray, the filtration units contained a 3D-printed seal and a perforated plate made of stainless steel. The perforated plate acted as a support structure during the solid-liquid separation [12]. Due to the identical external dimensions of the temperature control and filtration unit, any arrangement of the segments on the filter was possible. This allowed the kinetics of the overall process to be adjusted individually, which in turn enabled rapid adaptation to existing requirements. For example, if a model system was difficult to filtrate, it would be feasible to enlarge the solid-liquid separation zone by installing additional filtration units. Figure 3a,b depict detailed exploded drawings of the functional units.

Above the functional units was the filter medium. For this purpose, a monofilament cloth with a mesh size of 22 μm was used (SEFAR TETEX® MONO 07-76-SK 022, Sefar AG, Switzerland). To prevent any leakage of the solution due to capillary effects within the filter medium, a layer of liquid rubber was applied to the top and the bottom of the cloth (Flüssiggummi PUR, mibenco GmbH, Karlstein am Main, Germany). The contour of this layer corresponded to the shape of the process chamber. The filter cloth was attached to two plastic belts (IGAR GmbH & Co. KG, Offenbach am Main, Germany), whose teeth were partially replaced by metal carrier elements. To move the belts an electric motor was installed [12].

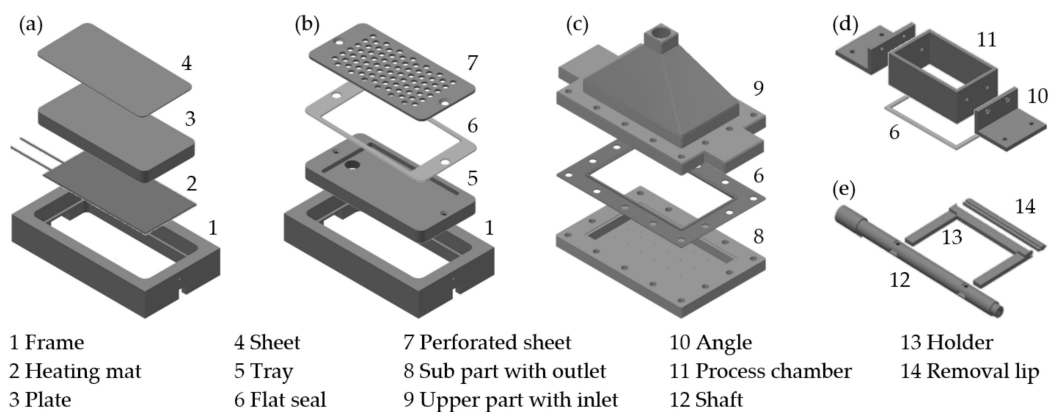


Figure 3. Exploded drawings. (a) Temperature control unit, (b) filtration unit, (c) cake washing device, (d) process chamber and (e) cake removal device.

The rectangular process chamber was on top of the filter medium. The underside of the component contained a seal. The two front sides were equipped with metal angles. For the exact positioning and transport of the process chamber, the angles were provided with holes matching the metal carrier elements of the toothed belts [12]. Figure 3d shows the general design of the process chamber.

In order to remove impurities from the filter cake, a device for cake washing was installed in the solid-liquid separation zone. The unit was made of a universally applicable upper part, a seal and a sub part that was individually adapted to the process parameters and the model system. To achieve a homogeneous distribution of the washing liquid over the entire outlet area, there was a flow divider inside the upper part. In addition, the bottom part had outlet cones that prevented the uncontrolled pooling of the escaping washing liquid. Figure 3c illustrates the entire element.

At the end of the belt section, the cake was removed from the filter. For this purpose, a scraper was integrated into the process. The device consisted of an aluminum shaft, a holder and a 3D-printed lip and can be taken from Figure 3e. The modular design of the scraper allowed variation of the removal angle as well as the changing of the material and geometry of the removal lip. Along with the easy replacement of damaged components, the tool offers a high degree of individuality and flexibility.

For cleaning the used filter medium, an aluminum wash tub was implemented. The tub was equipped with a separate inlet and outlet for the washing liquid and served to free the returning filter cloth from existing residues and deposits.

2.2. Particle System

The particulate system selected for the experimental studies was sucrose (Fein Zucker, Südzucker AG, Mannheim, Germany). The chemical connection was hydrolyzable by the absorption of water, which in turn ensured a high solubility. In order to determine the solubility of sucrose in water a correlation according to Vavrincz described in Mathlouthi and Reiser [17] is used in Equation (1). Herein, ϕ represents the solid mass fraction as function of the temperature T .

$$\phi = 64.47 + 8.222 \cdot 10^{-2} T + 1.6169 \cdot 10^{-3} T^2 - 1.558 \cdot 10^{-6} T^3 - 4.63 \cdot 10^{-8} T^4 \quad (1)$$

Another important physicochemical property is the dynamic viscosity η . The parameter is calculated to

$$\eta = 10^{A + \frac{B}{T + 273.15} + \frac{C}{T - 43.15}} \quad (2)$$

The coefficients, A , B and C and depend on the molar ratio of sucrose to water y and result in [18]

$$A = -2.038 - 13.627 y - 17.912 y^2 + 56.426 y^3, \quad (3)$$

$$B = 513.367 + 10,740.329 y - 16,781.321 y^2 + 14,142.897 y^3, \quad (4)$$

$$C = 16.993 + 34.442 y + 3915.947 y^2 - 6839.469 y^3 \quad (5)$$

The basis for all crystallization experiments (Sections 3.2–3.5) was 64.57 g of a sucrose solution saturated at 60 °C. For this purpose, 16.61 g ultrapure water and 47.96 g solid were mixed with a magnetic stirrer (RCT basic, IKA-Werke GmbH & Co. KG, Staufen, Germany) at a speed of 600 rpm for a time period of four hours. During the mixing process, the temperature was held at 65 °C to guarantee the complete dissolution of all particles. Immediately before the start of the experiment, the undersaturated solution was cooled to 60 °C and 0.13 g of seed crystals (Puderzucker fein, Südzucker AG, Mannheim, Germany) were added. The components were mixed for 60 s and fed into the process chamber located on the belt crystallizer.

2.3. Centrifugation Experiments

To characterize the crystals formed in the process, an optical centrifuge (LUMiSizer[®], LUM GmbH, Berlin, Germany) was used. The device measured the light transmission values at a wavelength of 865 nm and converted them into extinction profiles. The extinction values served as a foundation for the calculation of settling velocity and size distribution. Detloff et al. [19] gave a detailed explanation of the apparatus and the measuring principle.

The experiments performed in this study were all conducted at a speed of 1000 rpm, a temperature of 20 °C and a solids volume fraction of 0.008. To adjust this volume fraction, the sample taken from the process was diluted with a sucrose solution saturated at 20 °C. In order to calculate the amount of solution required for the dilution, it was assumed that the supersaturation within the sample had completely dissipated during the cooling process. The evaluation of the measurement data considered spherical particles with an equivalent diameter x_{eq} , which settled according to Stokes [20].

2.4. Filtration Experiments

A characteristic parameter in the field of filtration is the filtration resistance, which comprises the filter cake resistance r_c and the filter medium resistance R_M . To determine the resistance values, tests using a pressure nutsche were made. Thereby, a mixture of sucrose and ultrapure water with a solid mass fraction of 0.74 served as suspension. Within the scope of this work, both unused and used filter media were investigated. The used ones were contaminated close to the process by a crystallization experiment performed in advance on the surface of the filter cloth. VDI 2762 explained the principle test setup as well as the procedure and the analysis of the experiments [21].

For describing the filtration process, the equation of cake-forming filtration (Equation (6)) was used. The expression originates in Darcy's law and links the filtrate volume V with the concentration constant κ , dynamic viscosity η , filter area A , applied pressure difference Δp and the filtration resistances r_c and R_M [20].

$$\frac{t}{V} = \frac{\kappa \eta r_c}{2 A^2 \Delta p} V + \frac{\eta R_M}{A \Delta p} \quad (6)$$

The graphical application of Equation (6) results in a linear graph, where the ordinate intercept a allows the calculation of the filter medium resistance R_M following

$$R_M = a \frac{A \Delta p}{\eta} \quad (7)$$

In addition, the height-specific filter cake resistance r_c can be determined depending on the slope b by the formula

$$r_c = b \frac{2 A^2 \Delta p}{\kappa \eta} \quad (8)$$

Besides the tests with the pressure nutsche, filtration and demosturization experiments were performed on the belt crystallizer. To evaluate these studies, the solvent content sc into the filter cake was calculated according to

$$sc = \frac{m_{c,w} - m_{c,d}}{m_{c,w}} \quad (9)$$

The mass of the wet cake $m_{c,w}$ was measured immediately after the filtration process with a laboratory balance. To determine the dry mass $m_{c,d}$ the cake was then completely dehumidified in a drying oven at 60 °C and weighed again.

3. Results and Discussion

3.1. Commissioning of the Temperature Control Units in the Crystallization Zone

Initially, the focus was on the commissioning of the temperature control units in the crystallization zone. Considering that the temperature profile influences the supersaturation of the solution and thus also the properties of the resulting crystals, it is essential to be able to control the cooling curve during the particle formation process. Therefore, the aim of a first study is the realization of different temperature profiles [22]. For this purpose, the temperature of the solution was reduced from 60 to 20 °C within 1800 s in each case. To cool the solution, there were six temperature control units connected in series. The desired curves and the prevailing segment temperatures in the individual stages are given on the left hand side of Figure 4.

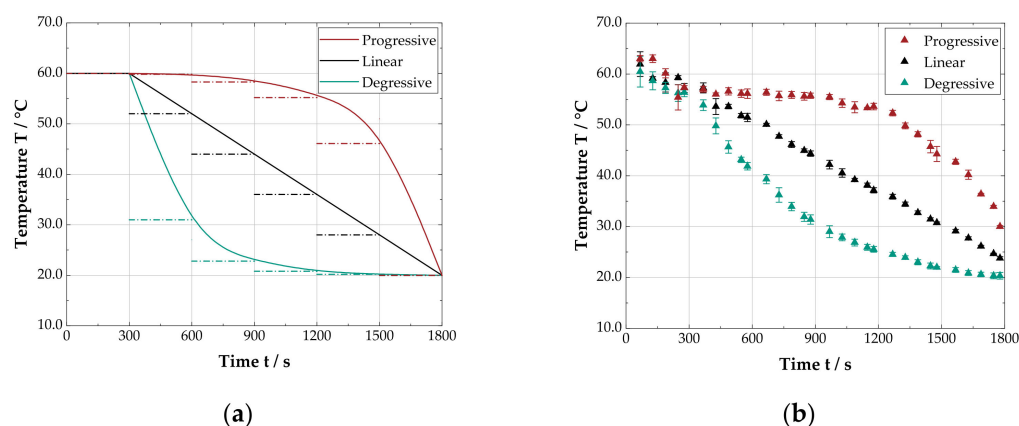


Figure 4. (a) Desired temperature curves of the solution (solid line) and temperature of the functional units (dot-dash) during progressive, linear and degressive cooling. The residence time per segment is 300 s. (b) Temperature of the solution at different cooling curves. While there is no deviation between the set and actual values at low to medium cooling rates, the high viscosity of the sucrose solution causes differences at high cooling rates.

The basis for the experimental tests was a sucrose solution with a solid mass fraction of 0.67. In order to determine the temperature, an infrared thermometer (5020-0385 Scan Temp 385, Dostmann electronic GmbH, Wertheim-Reicholzheim, Germany) allowed the measurement of the surface temperature of the solution at intervals of 60 s. The right side of Figure 4 shows the data obtained.

It is obvious that the cooling curve can be influenced and adjusted by the segment temperature. A good agreement between target and actual values is apparent at small to medium cooling rates below 8 °C per residence level. For temperature differences of more than 20 °C between two adjacent functional units, deviations from the target curve occur more frequently. This behavior appears, for example, at an early stage of the degressive curve and at an advanced stage of the progressive one. The existing differences result from the high viscosity of the solution and the inhibited heat conduction.

3.2. Influence of the Temperature Profile on the Crystal Properties

In the following, the influence of the temperature profile on the crystal properties is investigated in detail. The right side of Figure 4 indicates the temperature curves selected for the experiments. Directly after the cooling procedure, a representative sample of 500 μL was taken by means of a laboratory pipette (Research[®] plus, Eppendorf AG, Hamburg, Germany). Assuming the complete decomposition of the supersaturation, the suspension was diluted to a solid volume fraction of 0.008 and measured in the centrifugal field.

Figure 5 shows the determined cumulative particle size distributions. It is noticeable that the temperature curve influences the properties of the crystals. While degressive cooling produces rather small particles with the volume-based median diameter $x_{50,3} = 26.2 \pm 1.0 \mu\text{m}$, progressive temperature reduction forms particles with a diameter of $35.7 \pm 3.0 \mu\text{m}$. In the case of a linear temperature profile, the plant generates crystals with a size of $31.0 \pm 1.3 \mu\text{m}$. The differences result from the prevailing supersaturation in the system. In the progressive cooling process, the system is only slightly supersaturated at the beginning. This is why primarily crystal growth takes place. The growing rate is comparatively high due to the temperature, thus the particles enlarge rapidly. In contrast, the system is initially highly supersaturated in the case of a degressive progression. This in turn leads to an intensified nucleation instead of the growth of existing crystals. As a result, the median particle diameter is quite small.

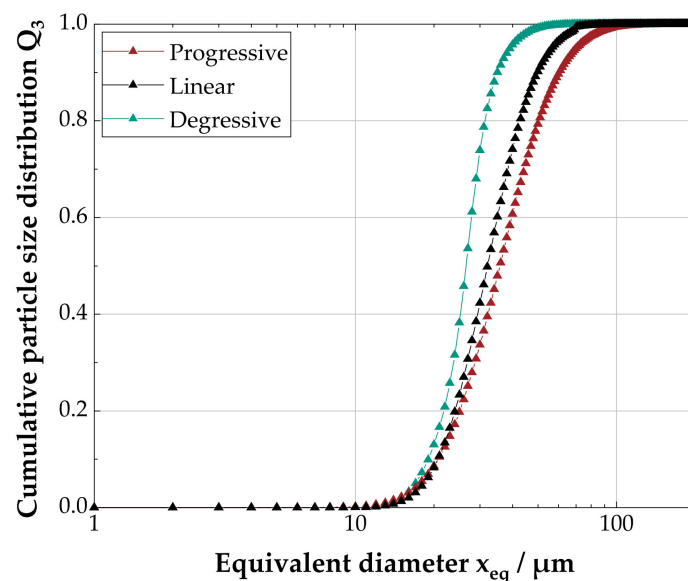


Figure 5. Particle size distribution of the crystals formed at different cooling curves, whereby the total process time is 1800 s in each case. The figure shows that the temperature profile clearly influences the crystal properties.

Apart from the particle size, the cooling curve also influences the distribution width. A characteristic parameter is the span, which links the particle sizes $x_{10,3}$, $x_{50,3}$ and $x_{90,3}$ and is given in Table 1. In the executed tests, the widest distribution (span = 1.1 ± 0.1) is obtained by a progressive cooling, whereas a degressive temperature profile results in a narrow distribution with a span of 0.6 ± 0.2 . Analogous to the median particle size, the distribution width for a linear ramp is between the progressive and the degressive cooling curves. Once again, the process conditions are responsible for the differences. The increasingly smaller temperature gradients during degressive cooling allow the uniform growth of the nuclei and the seed crystals. In contrast, in progressive cooling, the supersaturation ratio rises abruptly from a process time of approximately 1200 s onward. Hence, nucleation occurs, whereby small particles are formed and broaden the distribution.

Table 1. Median particle size and span at different cooling curves.

Cooling Curve	Median Particle Size	Span
	$x_{50,3}$ in μm	$(x_{90,3} - x_{10,3})/x_{50,3}$
Progressive	35.7 ± 3.0	1.1 ± 0.1
Linear	31.0 ± 1.3	0.9 ± 0.1
Degressive	26.2 ± 1.0	0.6 ± 0.2

3.3. Influence of Residence Time on the Crystal Properties

The properties of the particles are not only influenced by the temperature profile, but also by the residence time in the crystallization area. Consequently, further experiments focused on the investigation of this process parameter. Regardless of the selected residence time, a six-stage linear cooling took place in all cases. The temperatures prevailing in the individual stages were 60, 52, 44, 36, 28 and 20 °C. The residence time per segment varied from 300 to 900 s, resulting in overall times of 1800 to 5400 s. In order to analyze the manufactured crystals, measurements in the centrifugal field were carried out identically to Section 3.2.

Figure 6 shows the obtained particle size distributions. In principle, it can be seen that the particles become larger with increasing residence time. The median size is $31.0 \pm 1.3 \mu\text{m}$ at an interval of 300 s and increases to $43.8 \pm 4.5 \mu\text{m}$ when resting for 600 s. The largest particle diameter is reached at a duration of 900 s per functional unit. Here, the average particle size is $54.5 \pm 5.6 \mu\text{m}$.

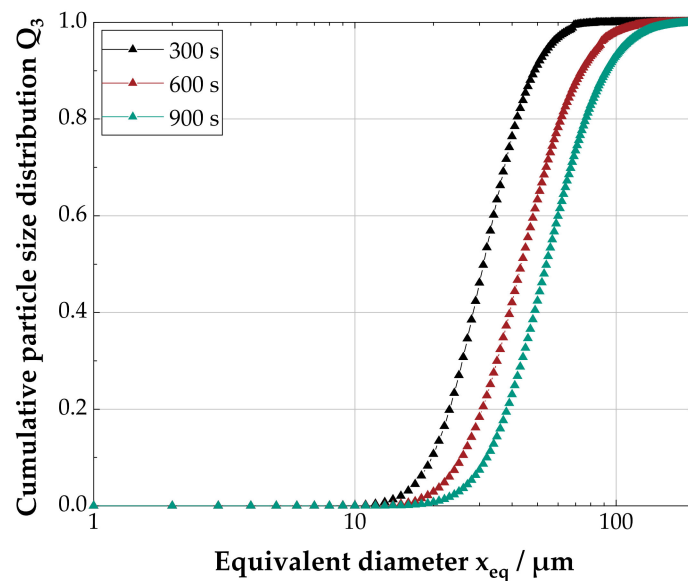


Figure 6. Particle size distribution during linear cooling as a function of the residence time. In principle, it can be seen that the formed particles become larger as the process time increases. The distribution width, however, remains almost constant.

Moreover, the experiments demonstrate that the residence time has only a marginal influence on the distribution width. The span assumes values between 0.9 and 1.0 and is within the range of the statistical deviation. The shift towards larger crystals with increasing crystallization time is due to longer growth and aging times, while the almost constant distribution width is a result of the similar cooling profiles.

3.4. Influence of the Crystallization Process on the Filter Medium

The three previous sections show that the laboratory plant is basically suitable for the production of particles by a cooling crystallization. To ensure that the crystallization process does not block the pores of the filter medium and thus greatly slow down or

completely prevent the subsequent solid-liquid separation, filtration tests were carried out on a pressure nutsche. In this context, the cloth was soiled close to the process and the filter medium resistance as well as the total resistance were determined. The total resistance is the sum of filter medium resistance and filter cake resistance, while the cake resistance is the product of the height specific cake resistance r_c and cake height h_c . Experiments in which an unused filter cloth was examined serve as reference. The calculated parameters and the relation of the averaged filter medium resistance to the mean total resistance can be found in Table 2.

Table 2. Calculated filtration resistances and ratio of the filter medium to total resistance.

Condition	Medium Resistance R_M in 10^9 m^{-1}	Total Resistance R in 10^9 m^{-1}	Ratio R_M/R
Unused	1.04 ± 0.36	10.05 ± 4.67	0.10
Used	1.97 ± 0.76	16.45 ± 5.00	0.12

The table indicates that the crystallization process tends to increase the filter medium resistance. The reason for this is an accumulation of crystals on or in the pores of the filter medium. To make these deposits visible, a laser-scanning microscope (Keyence VK-X 110, Keyence Deutschland GmbH, Germany) was used. Figure 7 depicts the captured images. The left side shows an unused filter cloth and the right side a soiled one.

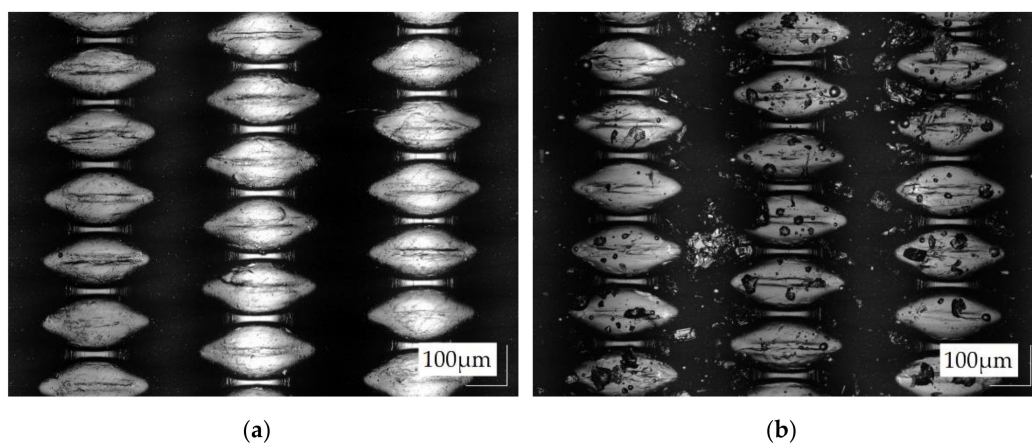


Figure 7. (a) Unused filter cloth. (b) Used filter cloth. On the surface of the used cloth there are crystalline structures, which increase the filter medium resistance.

To classify the results, a comparison of the averaged filter medium and total resistance is made. Thus, it becomes clear that the filter medium resistance only causes a small fraction (0.10 and 0.12) of the total resistance. According to this, it is possible to conclude that the increase in the filter medium resistance contains only a marginal and therefore negligible influence on the overall process.

In addition, washing tests occurred to investigate whether the contamination resulting from the crystallization was removable without any residues. For this purpose, the used filter medium was dropped in a 20 °C water bath for a time period of 300 s. Subsequent observation with a laser-scanning microscope revealed no crystals on the filter medium, so complete purification is expectable. Responsible for this residue-free cleaning is the high solubility of sucrose in the applied solvent.

3.5. Influence of the Desaturation Time on Filter Cake Properties

The solid-liquid separation area borders on the crystallization zone. Here, the solid and liquid components of the crystal suspension were separated from each other by an

applied pressure difference, resulting in the formation of a filter cake on the filter medium. Thereafter, the cake was mechanically demoistened.

The basis of the experiments was a crystal suspension generated by an 1800-s cooling process with a linear temperature profile. This was followed by 30 s of cake formation. The pressure difference was 800 mbar during both the cake formation and the consecutive desaturation. To determine the demoistening kinetics, the solvent content in the cake was detected.

Figure 8 shows that the solvent content sc in the cake is reduced from 0.13 to approximately 0.08 by mechanical desaturation. The decrease is almost exponential (dotted line) and corresponds to

$$sc = 0.079 + 0.049 e^{-0.01873 t} \quad (10)$$

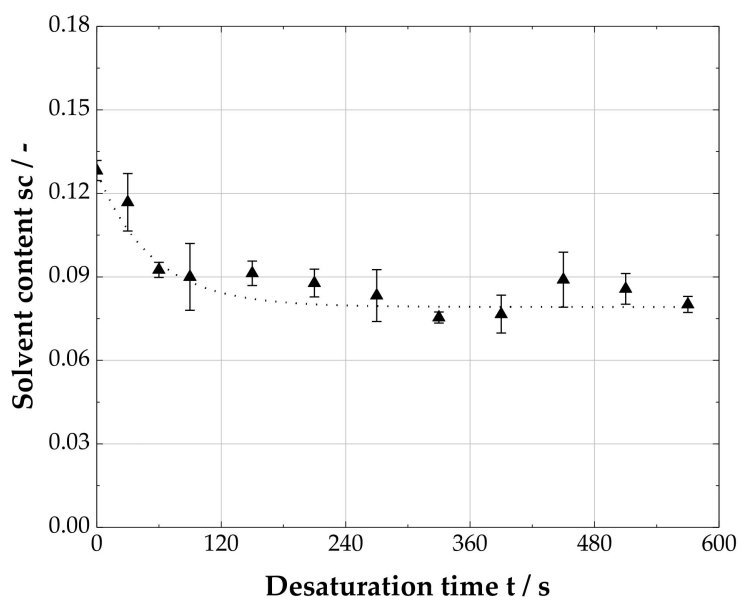


Figure 8. Solvent content in the filter cake as a function of the desaturation time. The figure shows that an almost steady-state value is reached after a short time, which makes a long demoisturization obsolete.

The equation enables the mathematical description and optimization of the solid-liquid separation step. It reveals that a state of equilibrium is reached in the filter cake after a short period of time, which makes a long demoisturization obsolete. From this point on, the solvent content can no longer be reduced mechanically but requires a post-process thermal drying [20].

4. Conclusions

An approach to meet the challenges in the chemical and pharmaceutical industry is the establishment of small, modular production plants with a high degree of automation and a wide range of applications. Based on that, this work presents an integrated apparatus concept for quasi-continuous particle synthesis and separation. The device combines the unit operations cooling crystallization, solid-liquid separation and drying in a single apparatus.

In addition to the development, the focus is on the commissioning of the plant. Thereby, the performed crystallization and filtration tests prove the general functionality of the system. The experiments demonstrate that the process parameters influence the properties of the produced particles. In this context, it is shown that the temperature profile during the cooling process influences both the particle size and the distribution width, and that larger crystals are formed as a result of a higher residence time in the crystallization zone. It is also found that the crystallization step slightly increases the resistance of the filter media. Compared to the overall resistance, however, this increase is marginal, which means that negative consequences for the overall process are not to be assumed.

Author Contributions: Conceptualization, T.D.; Data curation, T.D.; Formal analysis, T.D.; Funding acquisition, H.N.; Investigation, S.B.; Methodology, T.D.; Project administration, H.N.; Supervision, H.N.; Validation, T.D. and S.B.; Visualization, T.D.; Writing—original draft, T.D.; Writing—review and editing, T.D., M.G. and H.N. All authors have read and agreed to the published version of the manuscript.

Funding: The authors thank the German Federal Ministry for Economic Affairs and Energy for the financial support of this work. This research was made within the scope of the ENPRO initiative (support code: 03ET1652E). Furthermore, we acknowledge support by the KIT-Publication Fund of the Karlsruhe Institute of Technology.

Data Availability Statement: Not applicable.

Conflicts of Interest: The authors have declared no conflict of interest.

References

1. Lier, S.; Wörsdörfer, D.; Grünewald, M. Wandlungsfähige Produktionskonzepte: Flexibel, Mobil, Dezentral, Modular, Beschleunigt. *Chem. Ing. Tech.* **2015**, *87*, 1147–1158. [[CrossRef](#)]
2. Bieringer, T.; Buchholz, S.; Kockmann, N. Future Production Concepts in the Chemical Industry: Modular—Small-Scale—Continuous. *Chem. Eng. Technol.* **2013**, *36*, 900–910. [[CrossRef](#)]
3. Lang, J.; Stenger, F.; Schütte, R. Chemieanlagen der Zukunft—Unikate und/oder Module. *Chem. Ing. Tech.* **2012**, 883–884. [[CrossRef](#)]
4. Lier, S.; Paul, S.; Ferdinand, D.; Grünewald, M. Modulare Verfahrenstechnik: Apparateentwicklung für wandlungsfähige Produktionssysteme. *Chem. Ing. Tech.* **2016**, *88*, 1444–1454. [[CrossRef](#)]
5. Seifert, T.; Sievers, S.; Bramsiepe, C.; Schembecker, G. Small scale, modular and continuous: A new approach in plant design. *Chem. Eng. Process. Process. Intensif.* **2012**, *52*, 140–150. [[CrossRef](#)]
6. Fleischer, C.; Wittmann, J.; Kockmann, N.; Bieringer, T.; Bramsiepe, C. Sicherheitstechnische Aspekte bei Planung und Bau modularer Produktionsanlagen. *Chem. Ing. Tech.* **2015**, *87*, 1258–1269. [[CrossRef](#)]
7. Reitze, A.; Jürgensmeyer, N.; Lier, S.; Kohnke, M.; Riese, J.; Grünewald, M. Auf dem Weg zur Smart Factory: Modulare, intelligente Konzepte für die Produktion von Spezialchemikalien der Zukunft. *Angew. Chem.* **2018**, *130*, 4318–4324. [[CrossRef](#)]
8. VDI-Gesellschaft Verfahrenstechnik und Chemieingenieurwesen. *Process Engineering Plants—Modular Plants—Fundamentals and Planning Modular Plants*; Beuth Verlag GmbH: Berlin, Germany, 2020.
9. Hohmann, L.; Kössl, K.; Kockmann, N.; Schembecker, G.; Bramsiepe, C. Modules in process industry—A life cycle definition. *Chem. Eng. Process. Process. Intensif.* **2017**, *111*, 115–126. [[CrossRef](#)]
10. Baldea, M.; Edgar, T.F.; Stanley, B.L.; Kiss, A.A. Modular manufacturing processes: Status, challenges, and opportunities. *AIChE J.* **2017**, *63*, 4262–4272. [[CrossRef](#)]
11. Bieringer, T.; Bramsiepe, C.; Brand, S.; Brodhagen, A.; Dreiser, C.; Fleischer-Trebes, C.; Kockmann, N.; Lier, S.; Schmalz, D.; Schwede, C.; et al. *Modulare Anlagen: Flexible Chemische Produktion durch Modularisierung und Standardisierung—Status quo und zukünftige Trends*; DECHEMA e.V.: Frankfurt, Germany, 2017.
12. Löbnitz, L. *Auslegung des Separationsprozesses und Entwicklung Neuer Verfahrenskonzepte zur Integrierten Produktion und Separation Kristalliner Aminosäuren*; Karlsruher Institut für Technologie: Karlsruhe, Germany, 2020.
13. Gehrman, D.; Schweigler, N. Device for Continuous Filtration and Drying of a Solid Suspension. U.S. Patent No. 5,527,458, 18 June 1996.
14. Schweigler, N.; Gehrman, D.; Bamberger, T.; Tichy, J. Kontinuierliche Filtration und Trocknung auf einem neuartigen Filtertrockner (Konfilitro). *Chem. Ing. Tech.* **1995**, *67*, 1186–1187. [[CrossRef](#)]
15. Thurner, F. Der Titus-Nutsch-Trockner—Neue Wege der Produktisolierung. *Chem. Ing. Tech.* **1990**, *62*, 753–755. [[CrossRef](#)]
16. Capellades, G.; Neurohr, C.; Azad, M.; Brancazio, D.; Rapp, K.; Hammersmith, G.; Myerson, A.S. A Compact Device for the Integrated Filtration, Drying, and Mechanical Processing of Active Pharmaceutical Ingredients. *J. Pharm. Sci.* **2020**, *109*, 1365–1372. [[CrossRef](#)] [[PubMed](#)]
17. Mathlouthi, M.; Reiser, P. *Sucrose: Properties and Applications*; Springer US: Boston, MA, USA, 1995.
18. Pot, A. *Industrial Sucrose Crystallisation: A Study on the Development of Crystal Size Distributions in Continuous and Batch Sucrose Suspension Crystallisers*; Technische Universität Delft: Delft, The Netherlands, 1983.
19. Detloff, T.; Sobisch, T.; Lerche, D. Particle Size Distribution by Space or Time Dependent Extinction Profiles obtained by Analytical Centrifugation. *Part. Part. Syst. Charact.* **2006**, *23*, 184–187. [[CrossRef](#)]
20. Anlauf, H. *Wet Cake Filtration: Fundamentals, Equipment, Strategies*; WILEY VCH: Weinheim, Germany, 2020.
21. VDI-Gesellschaft Verfahrenstechnik und Chemieingenieurwesen. *Mechanical Solid-Liquid Separation by Cake Filtration—Determination of Filter Cake Resistance*; Beuth Verlag GmbH: Berlin, Germany, 2010.
22. Elahi, M. *Untersuchungen zur Optimierung der Kühlrate der Kühlungskristallisation von Nachprodukt-Kristallsuspensionen bei der Saccharosegewinnung*; Technische Universität Berlin: Berlin, Germany, 2004.